Probing the correlation between ligand efficacy and conformational diversity at the α_{1A}-adrenoreceptor reveals allosteric coupling of its microswitches

Feng-Jie Wu[1,2,3], Lisa M. Williams[3], Alaa Abdul-Ridha[3], Avanka Gunatilaka[3], Tasneem M. Vaid[1,2,3], Martina Kocan[3], Alice R. Whitehead[3], Michael D.W. Griffin[1,2], Ross A.D. Bathgate[1,3], Daniel J. Scott[1,3*], Paul R. Gooley[1,2*]

From the [1]Department of Biochemistry and Molecular Biology, University of Melbourne, Parkville, 3052, VIC, Australia; [2]Bio21 Molecular Science and Biotechnology Institute, University of Melbourne, Parkville, 3052, VIC, Australia; [3]The Florey Institute of Neuroscience and Mental Health, University of Melbourne, Parkville, 3052, VIC, Australia.

Running title: *Correlation of conformation with ligand efficacy for α_{1A}-AR*

*To whom correspondence should be addressed: Paul R. Gooley, Department of Biochemistry and Molecular Biology, The University of Melbourne Bio21 Molecular Science and Biotechnology Institute,Phone: +61 (0)3 8344 2273, Email: prg@unimelb.edu.au; Daniel J. Scott, The Florey Institute of Neuroscience and Mental Health, The University of Melbourne, Phone: +61 (0)3 9035 7584, Email: daniel.scott@florey.edu.au.

SUPPORTING INFORMATION

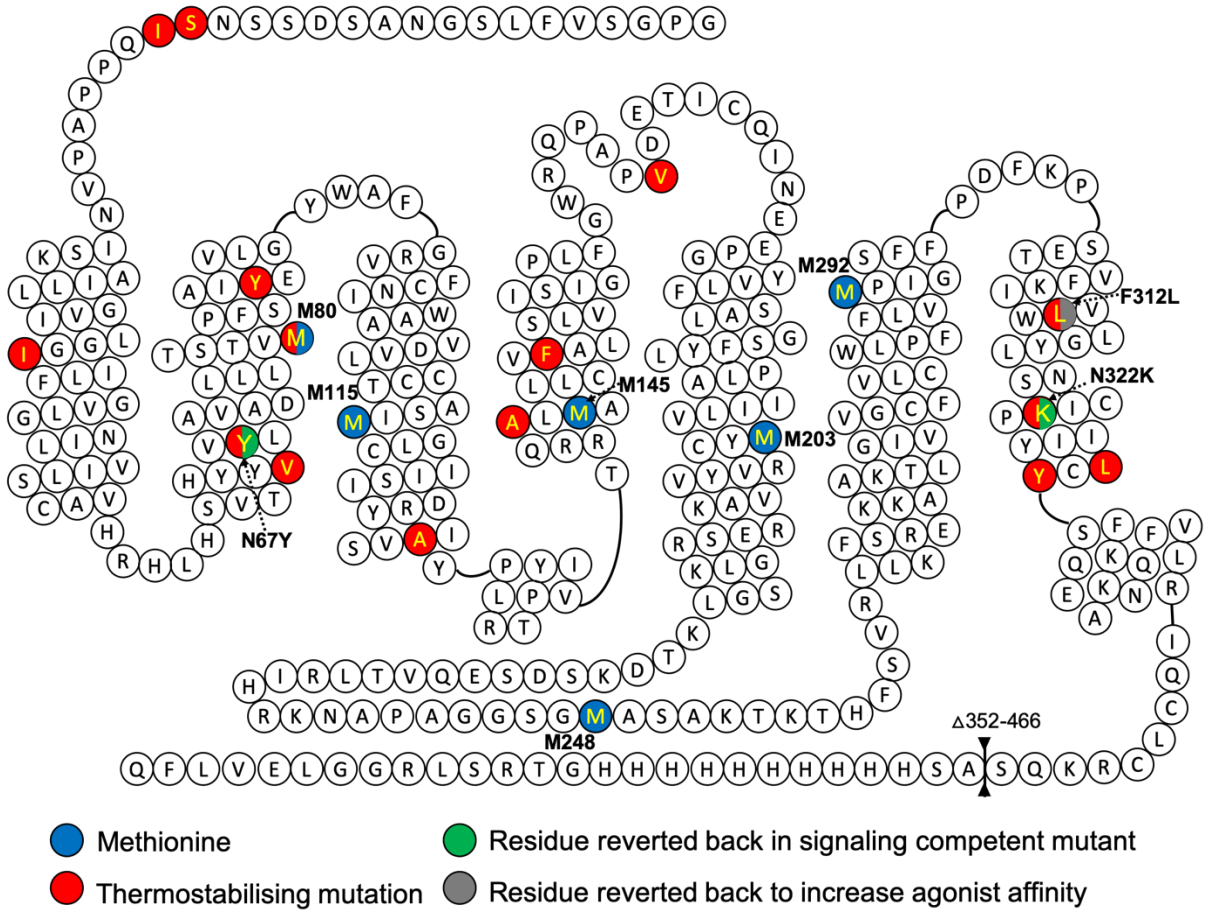

Figure S1. Secondary structure diagram of human α_{1A}-AR-A4. Methionine residues and thermostabilisation mutations are labelled in blue and red, respectively. Two thermostabilisation mutations (N67Y, N322K) labelled in both red and green were reverted back to natural residues in making signaling competent construct α_{1A}-AR-A4-active (Y67N, K322N). Residue labelled in grey is critical for ligand binding, α_{1A}-AR-A4 (L312F) construct was made to rescue affinities of agonists tested in this study.

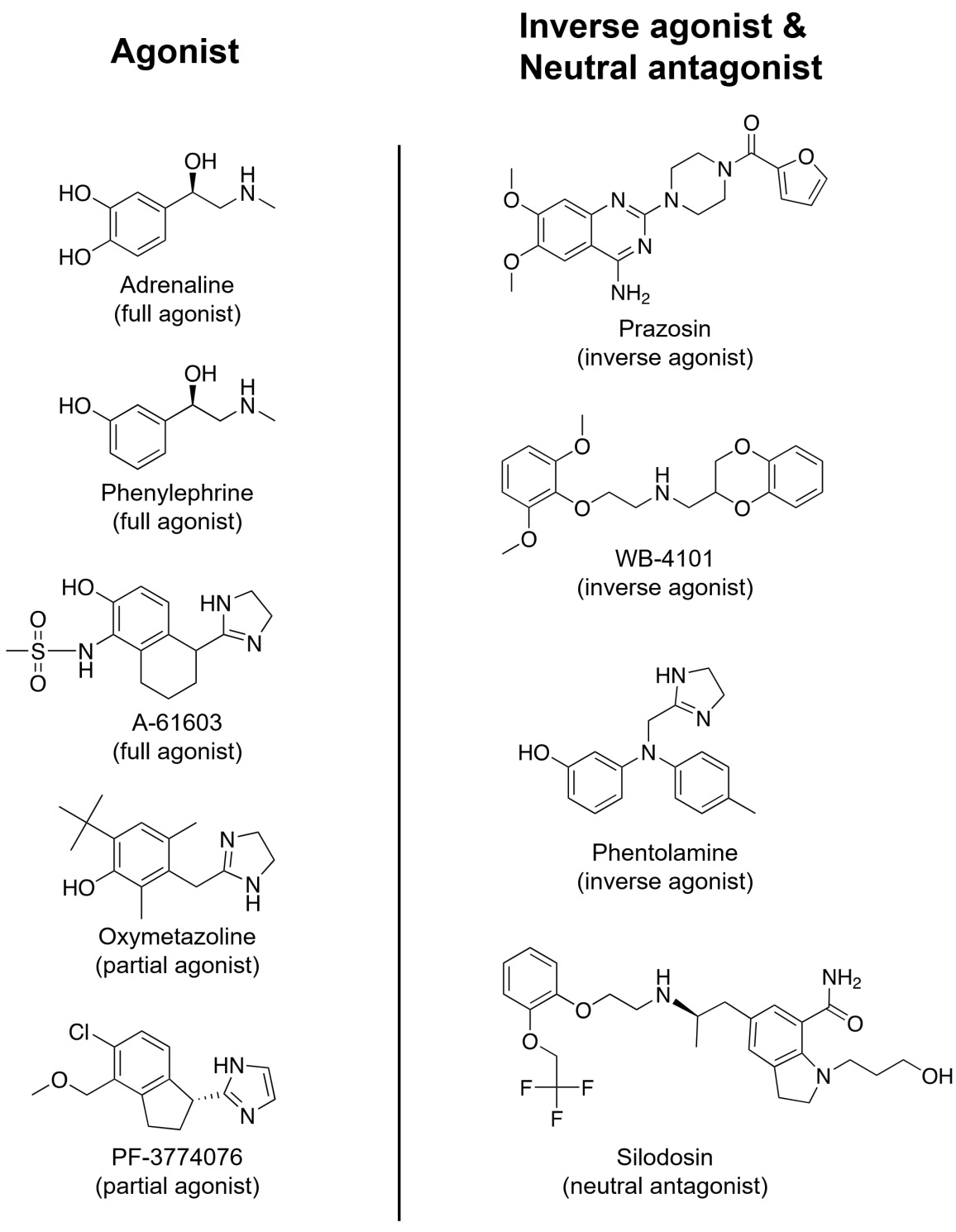

Figure S2. Chemical structures of ligands used in this study.

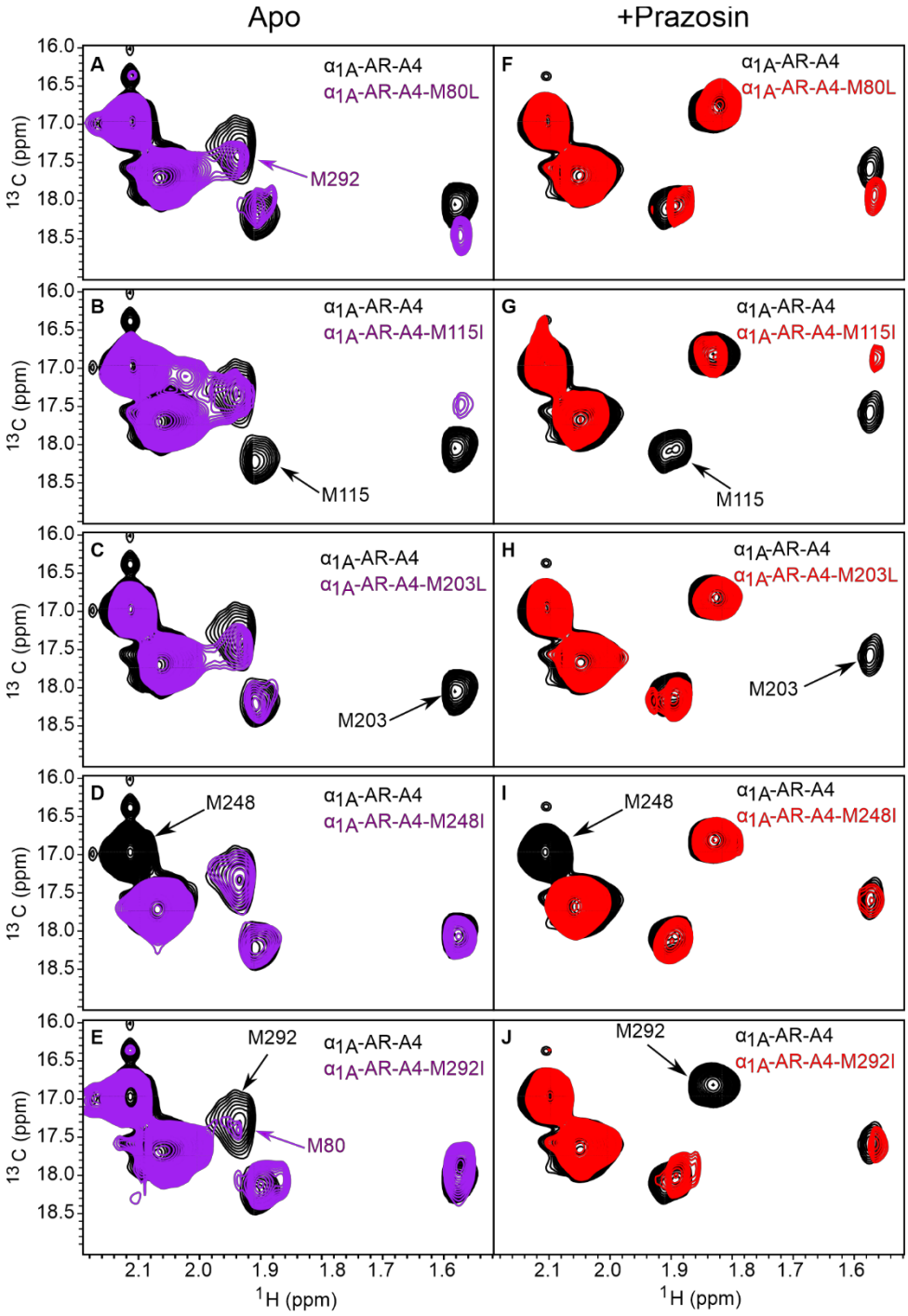

Figure S3. Assignment of ^{13}C methyl labelled methionine residues in α_{1A}-AR-A4. Five methionine residues in α_{1A}-AR-A4 were individually mutated to either Leucine or Isoleucine, M80L (A,F); M115I (B,G); M203L (C,H); M248I (D,I); M292I (E,J). The ^{1}H-^{13}C SOFAST HMQC spectra of five α_{1A}-AR-A4 mutants were collected in apo state (a-e, purple) and prazosin-bound state (F-J, red). Spectra of all mutants overlay with the spectrum of α_{1A}-AR-A4 in the apo or prazosin-bound state (black).

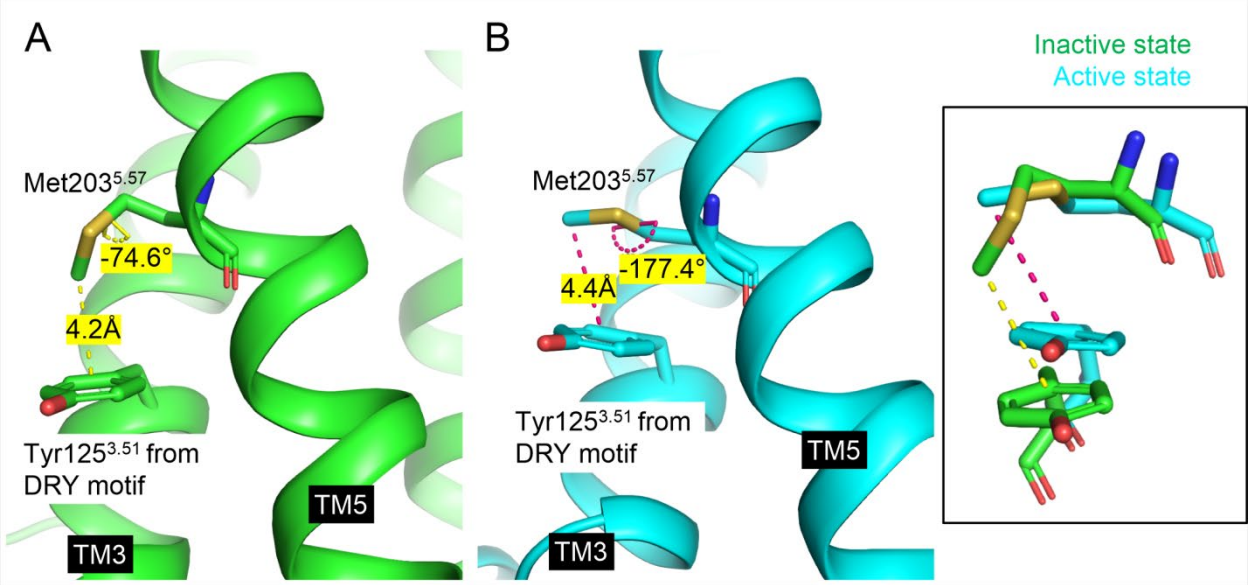

Figure S4. The local environment of Met203$^{5.57}$ and its χ3 dihedral angle.
The methyl group of Met203$^{5.57}$ sits on top of Tyr125$^{3.51}$ of the DRY motif as shown in the α_{1A}-AR-A4 homology models, and is expected to experience a ring current effect from Tyr125$^{3.51}$. (A) In the inactive state of α_{1A}-AR-A4 model (green), the distance between the methyl of Met203$^{5.57}$ and the ring of Tyr125$^{3.51}$ is 4.2Å. The χ3 dihedral angle of Met203$^{5.57}$ is -74.6º, which means the χ3 in the inactive state is averaging between gauche and trans conformers. (B) In the active state of α_{1A}-AR-A4 model (cyan), the distance between the methyl of Met203$^{5.57}$ and the ring of Tyr125$^{3.51}$ is 4.4Å. The χ3 dihedral angle of Met203$^{5.57}$ is -177.4º, which means the χ3 in the active state is in a near trans conformer.

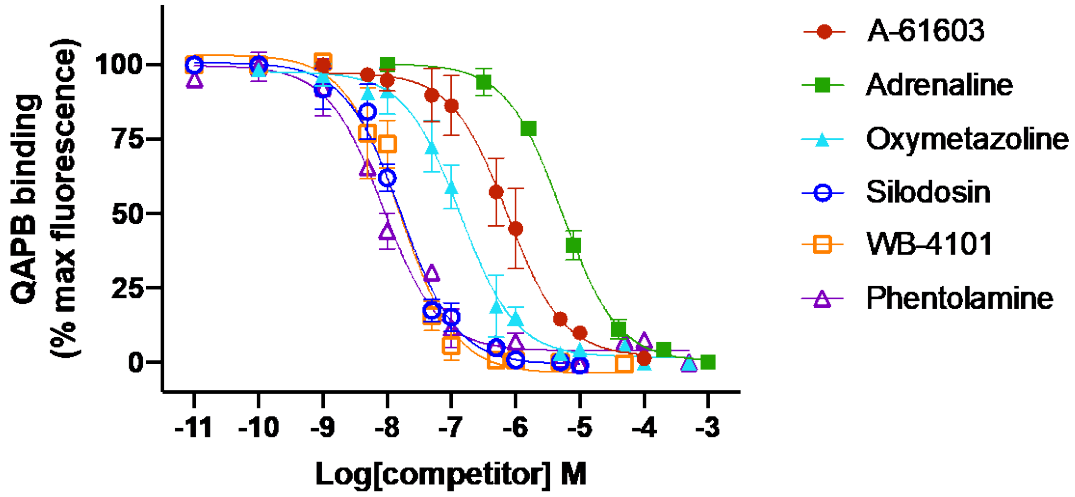

Figure S5. Characterisation of ligand affinity to α_{1A}-AR-A4 (L312F). QAPB competition binding for 2 hours at 22 °C against purified α_{1A}-AR-A4 (L312F) with A-61603 (maroon, solid circles), adrenaline (green, solid squares), oxymetazoline (cyan, solid triangles), silodosin (blue, open circles), WB-4101 (orange, open squares) and phentolamine (purple, open triangles).

Table S1. Measured affinities of ligands utilised in the present study.[a]

	α_{1A}-AR WT	α_{1A}-AR-A4	α_{1A}-AR-A4 (L312F)	α_{1A}-AR-A4-active
QAPB K_D (nM)	N.D	11.6 ± 2.0[1]	30.3 ± 21.2	29.2 ± 15.1
	K_i[b]	K_i	K_i	K_i
Adrenaline	3.3 ± 0.4 μM[2]	>1.0 mM[1]	2.7 ± 0.5 μM	0.4 ± 0.1 mM
Phenylephrine	6.2 ± 1.5 μM[2]	~0.6 mM[1]	41.9 ± 26.6 μM[1]	1.6 ± 0.6 mM
A-61603	~79.4 nM[3]	113.5 ± 47.2 μM[1]	0.4 ± 0.2 μM	18.4 ± 18.9 μM
Oxymetazoline	6.7 ± 0.9 nM[4]	52.8 ± 8.0 μM	65.7 ± 24.4 nM	9.7 ± 6.4 μM
PF-3774076	~83.0 nM[5]	N.D	N.D	19.4 ± 12.9 μM
Silodosin	0.036 ± 0.010 nM[4]	N.D	8.4 ± 1.9 nM	5.9 ± 0.7 nM
Phentolamine	2.7 ± 0.1 nM[4]	N.D	3.9 ± 2.0 nM	623.4 ± 162.6 nM
WB-4101	0.21 ± 0.03 nM[4]	N.D	7.6 ± 3.4 nM	269.0 ± 108.7 nM
Prazosin	0.17 ± 0.02 nM[4]	57.0 ± 11.8 nM[1]	7.5 ± 3.8 nM[1]	61.9 ± 50 nM

[a] Data are presented as mean K_i ± SD and mean K_D ± SD, except for the data cited from the literature which are mean K_i ± SEM and mean K_D ± SEM. Three independent biological replicate experiments (n=3) were done for all data. N.D, not determined. [b]These K_i were measured on cells overexpressed with WT human α_{1A}-AR. K_i of ligands on α_{1A}-AR-A4, α_{1A}-AR-A4 (L312F) and α_{1A}-AR-A4-active were determined with purified receptors using Kingfisher binding assay (see methods). For some ligand-receptor pairings, full displacement in competition binding assays was not observed, and thus only approximate K_i values could be estimated (indicated with ~).

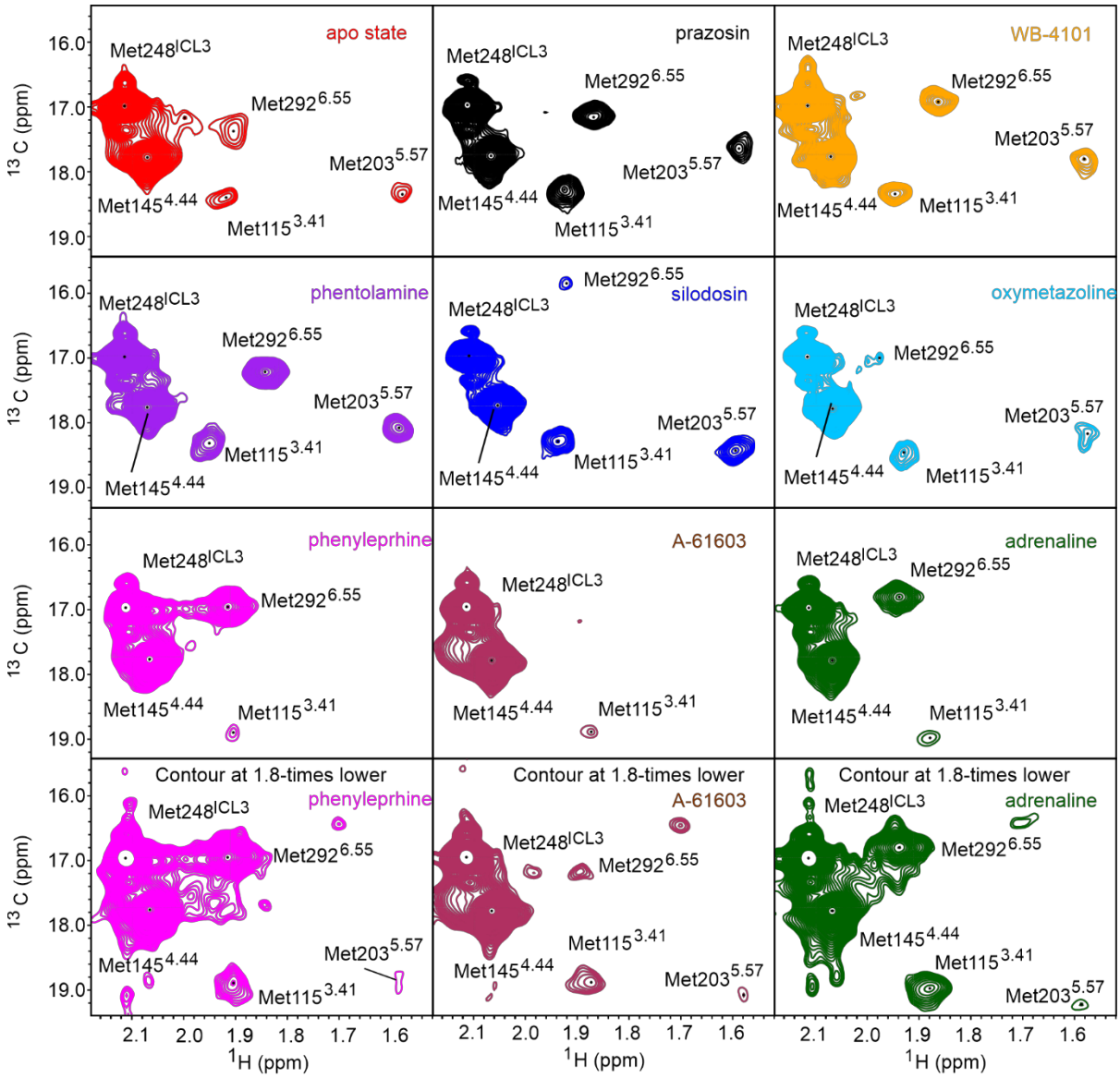

Figure S6. **^{1}H-^{13}C SOFAST-HMQC spectra of α_{1A}-AR-A4 (L312F).** Individual NMR spectrum for [$^{13}C^{\varepsilon}H_3$-Met] α_{1A}-AR-A4 (L312F) collected in the apo-state (red) and bound to prazosin (black, inverse agonist), WB-4101 (yellow, inverse agonist), phentolamine (purple, inverse agonist), silodosin (blue, neutral antagonist), oxymetazoline (cyan, partial agonist), phenylephrine (magenta, full agonist), A-61603 (maroon, full agonist), and adrenaline (green, full agonist).

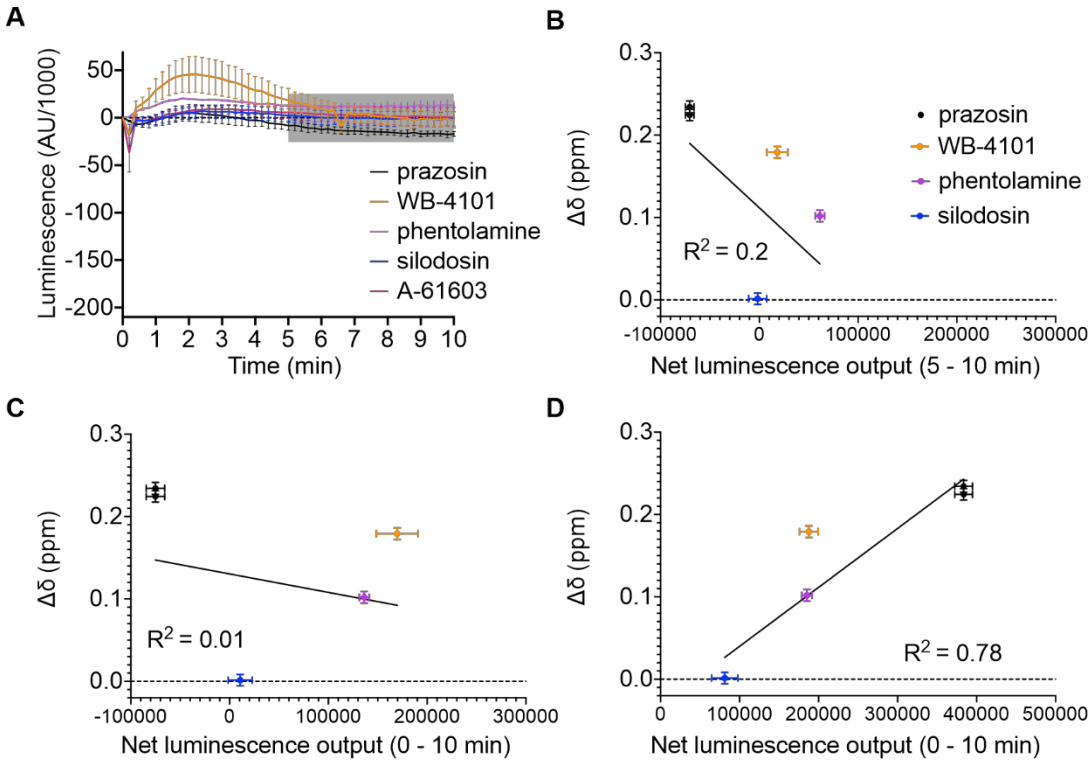

Figure S7. **Controls for NanoBit G protein activity assay.** (A) NanoBit G protein activity assay on empty vector (pcDNA3.1/Zeo) transfected COS-7 cells treated with the same concentrations of prazosin, WB-4101, phentolamine and silodosin as in Figure 4B. The grey shaded region indicates where the area under the curve measurements were taken for (B). (B) Linear regression analysis of the average chemical shift differences (Δδ) for the $^{13}C^{\varepsilon}H_3$ of Met203 in α_{1A}-AR-A4 (L312F) and the increase in luminescence seen between 5 – 10 min after treatment in the NanoBit assay on empty vector (pcDNA3.1/Zeo) transfected COS-7 cells. A P value of 0.2663 was obtained when testing against the null hypothesis of a slope of 0 (C) Linear regression analysis of the average chemical shift differences (Δδ) for the $^{13}C^{\varepsilon}H_3$ of Met203 in α_{1A}-AR-A4 (L312F) and the increase in luminescence seen for the first 10 min after treatment in the NanoBit assay on empty vector (pcDNA3.1/Zeo) transfected COS-7 cells. Ligands are coloured as listed above and a P value of 0.6754 indicated slope not deviating significantly from 0. (D) Linear regression analysis of the average chemical shift differences (Δδ) for the $^{13}C^{\varepsilon}H_3$ of Met203 in α_{1A}-AR-A4 (L312F) and the increase in luminescence seen for the first 10 min after treatment in the NanoBit assay on COS-7 cells transfected with wild-type α_{1A}-AR (as in Figure 4B-C). A P value of 0.0071 suggested a significantly non-zero slope. Ligands are coloured as listed above. In (B), (C) and (D) Δδ are plotted for two independent titrations of prazosin and silodosin, and single experiments for WB-4101 and phentolamine. Average chemical shift differences (Δδ) were normalised using the equation $\Delta\delta=[(\Delta\delta_{1H})^2+(\Delta\delta_{13C}/3.5)^2]^{0.5}$ and errors were calculated by the formula $|[\Delta\delta_{1H}*R_{1H}+\Delta\delta_{13C}*R_{13C}/(3.5)^2]|/\Delta\delta$, where R_{1H} and R_{13C} are the digital resolutions in ppm in the ^{1}H and ^{13}C dimensions respectively.

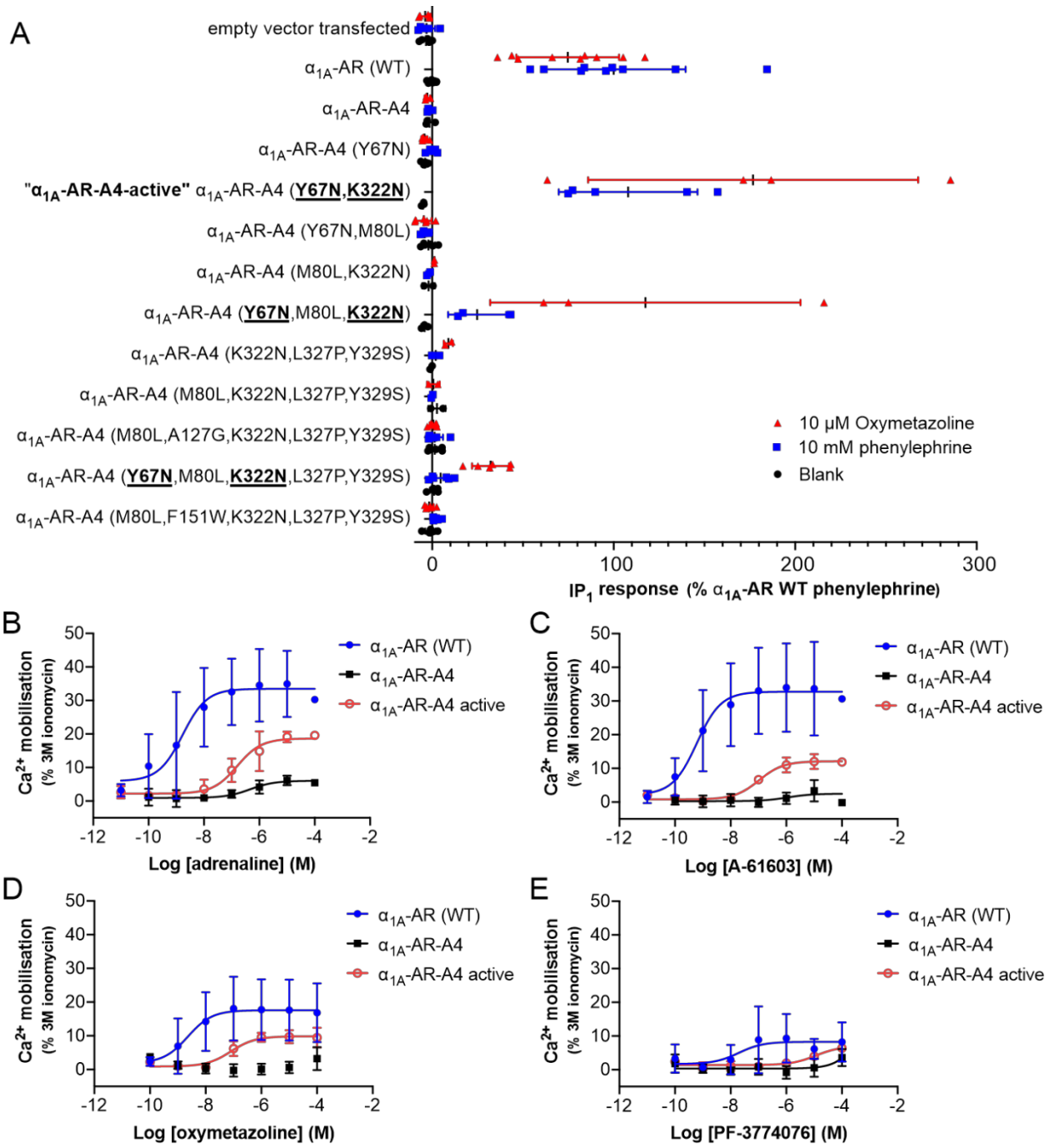

Figure S8. Functional signalling assays performed on α_{1A}-AR-A4 active and other mutants. (A) Screening of agonist (phenylephrine and oxymetazoline) induced accumulation of IP_1 in COS-7 cells transfected with WT α_{1A}-AR, α_{1A}-AR-A4. This assay should be treated as a qualitative measure of receptor function. Mutants that were made with reverted mutations on α_{1A}-AR-A4. Y67N, M80L, A127G, F151W, K322N, L327P and Y329S are the predicted critical back mutations that were screened to recover the signaling ability of α_{1A}-AR-A4. All of α_{1A}-AR-A4 back mutants containing Y67N and K322N (highlighted with bold and underlined) displayed accumulation of IP_1 signal upon agonist activation. α_{1A}-AR-A4 (Y67N, K322N) is labelled as α_{1A}-AR-A4-active. In this screening assay some mutants were only measured in one biological

replicate experiment (α_{1A}-AR-A4 (M80L,K322N,L327P,Y329S; α_{1A}-AR-A4 (K322N,L327P,Y329S); α1A-AR-A4 (Y67N,M80L,K322N); α_{1A}-AR-A4 (M80L,K322N); α_{1A}-AR-A4 (Y67N,K322N); α_{1A}-AR-A4), with the others measured in two independent biological replicate experiments, with data plotted as mean ± SD of replicate measurements. (B-E) Measurement of adrenaline (B), A-61603 (C), oxymetazoline (D) and PF-3774076 (E) induced Ca^{2+} mobilization in COS-7 cells transfected with α_{1A}-AR (blue, solid circles), α_{1A}-AR-A4 (black, solid squares) and α_{1A}-AR-A4 active (red, open circles). Data represent the mean ± SD from three independent biological replicate experiments, each measured as three technical replicates.

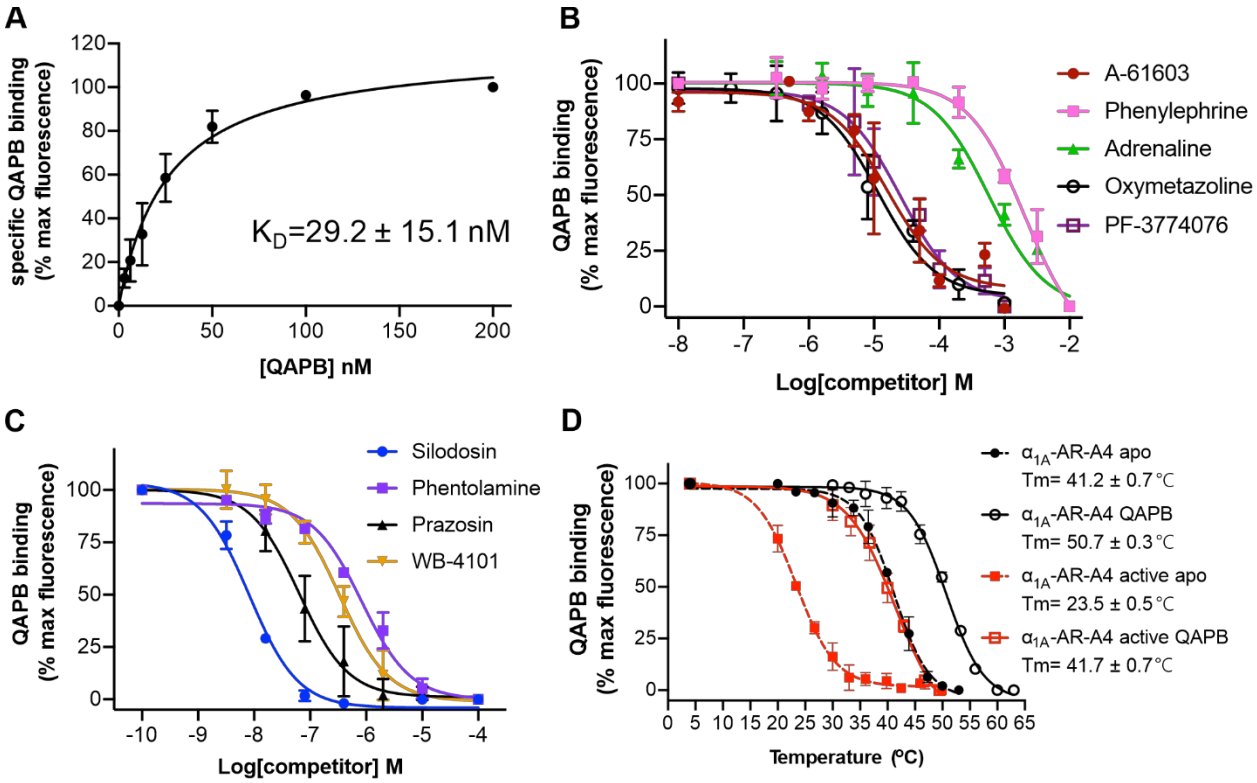

Figure S9. Characterisation of α_{1A}-AR-A4-active. (a) Saturation binding of QAPB to purified α_{1A}-AR-A4 active. (b) QAPB competition binding for 2 hours at 22 °C against purified α_{1A}-AR-A4 active with different agonists. (c) QAPB competition binding for 2 hours at 22 °C against purified α_{1A}-AR-A4 active with antagonist and inverse agonists. (d) Thermostability assay performed on α_{1A}-AR-A4 in the apo state (black solid circles and dash line), QAPB-bound state (black open circles and solid line) and α_{1A}-AR-A4-active in the apo state (red solid squares and dash line), QAPB-bound state (red open squares and solid line).

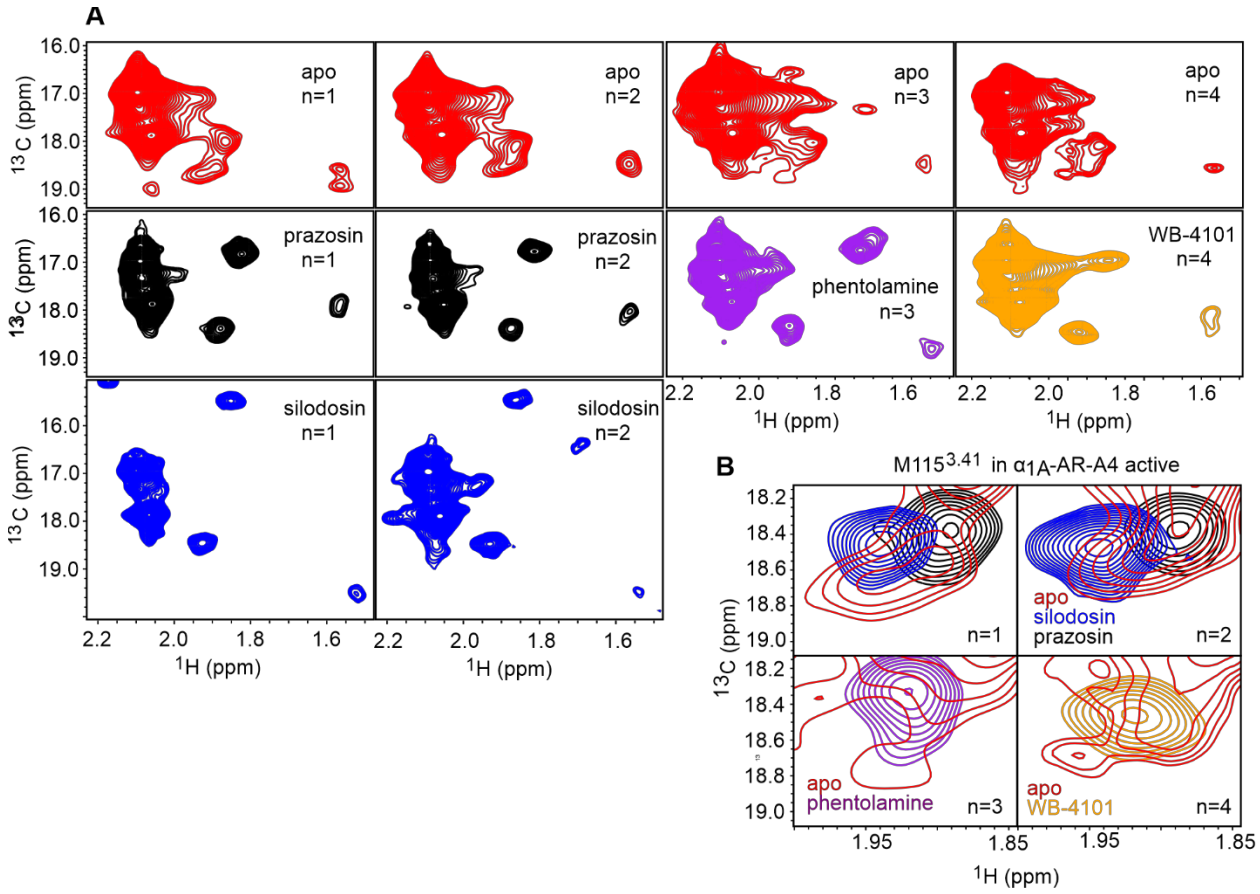

Figure S10. **^{1}H-^{13}C SOFAST-HMQC spectra of α_{1A}-AR-A4-active.** (A) Four separate expressions and purifications of α_{1A}-AR-A4-active were conducted and data acquired for apo- (red), prazosin (black) and silodosin (blue), phentolamine (purple) and WB-4101 (orange). (B) Expansions and overlay of the region where the $^{13}C^{\varepsilon}H_3$ of Met115 resonates.

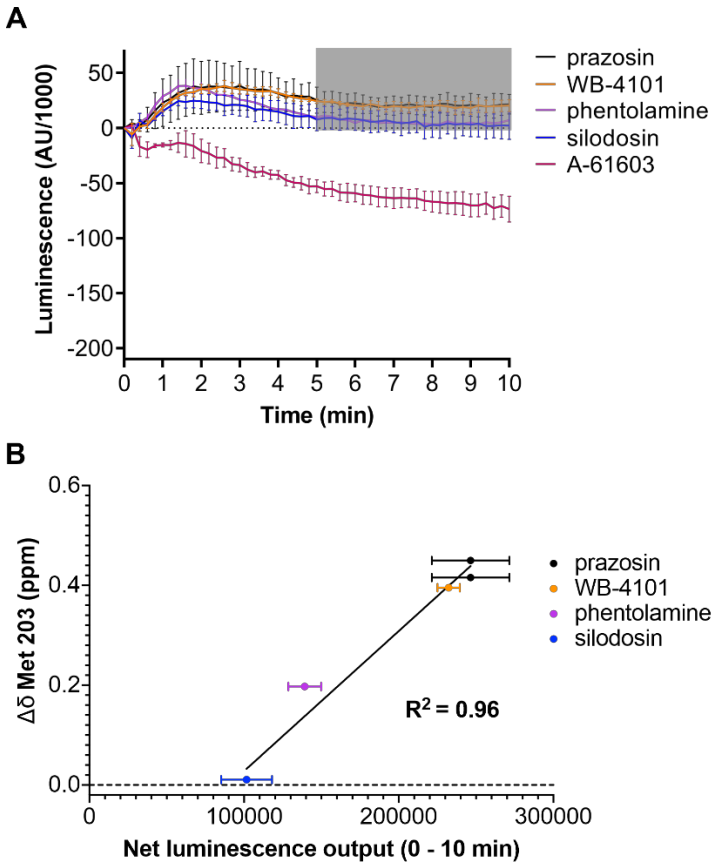

Figure S11. **Correlation between the chemical shift position of Met203$^{5.57}$ in α_{1A}-AR-A4-active and inverse agonists efficacy.** (A) NanoBit G protein activity assay demonstrating inverse agonism of prazosin, WB-4101, phentolamine and silodosin at α_{1A}-AR-A4 active expressing COS-7 cells. The grey shaded region indicates where the area under the curve measurements were taken to make Figure 5e. (b) Linear regression analysis of the average chemical shift differences (Δδ) for the $^{13}C^{\varepsilon}H_3$ of Met203 in α_{1A}-AR-A4-active and the increase in luminescence seen over the first 10 minutes in the NanoBit assay for each antagonist. A P value of 0.0002 suggested that the slope was significantly different from zero. In (B) Δδ are plotted for two independent titrations of prazosin and silodosin, and single experiments for WB-4101 and phentolamine. Average chemical shift differences (Δδ Met 203) were normalised using the equation $\Delta\delta=[(\Delta\delta_{1H})^2+(\Delta\delta_{13C}/3.5)^2]^{0.5}$ and errors were calculated by the formula $|[\Delta\delta_{1H}*R_{1H}+\Delta\delta_{13C}*R_{13C}/(3.5)^2]|/\Delta\delta$, where R_{1H} and R_{13C} are the digital resolutions in ppm in the ^{1}H and ^{13}C dimensions respectively.

Reference

1. Yong, K.J. et al. Determinants of Ligand Subtype-Selectivity at alpha1A-Adrenoceptor Revealed Using Saturation Transfer Difference (STD) NMR. *ACS Chem Biol* **13**, 1090-1102 (2018).
2. Hwa, J. & Perez, D.M. The unique nature of the serine interactions for alpha 1-adrenergic receptor agonist binding and activation. *Journal of Biological Chemistry* **271**, 6322-6327 (1996).
3. Willems, E.W. et al. A61603-induced vasoconstriction in porcine carotid vasculature: involvement of a non-adrenergic mechanism. *Eur J Pharmacol* **417**, 195-201 (2001).
4. Shibata, K. et al. KMD-3213, a novel, potent, alpha 1a-adrenoceptor-selective antagonist: characterization using recombinant human alpha 1-adrenoceptors and native tissues. *Mol Pharmacol* **48**, 250-8 (1995).
5. Conlon, K. et al. Pharmacological properties of 2-((R-5-chloro-4-methoxymethylindan-1-yl)-1H-imidazole (PF-3774076), a novel and selective alpha1A-adrenergic partial agonist, in in vitro and in vivo models of urethral function. *J Pharmacol Exp Ther* **330**, 892-901 (2009).